Transonic flow simulation in a bent channel using SU2 software

1st Anatoly Ryabinin
Department of Hydroaeromechanics
Saint Petersburg University
Saint Petersburg, Russia
a.ryabinin@spbu.ru

2nd Alexander Kuzmin
Department of Hydroaeromechanics
Saint Petersburg University
Saint Petersburg, Russia
a.kuzmin@spbu.ru

***Abstract*—Turbulent 2D airflow in a bent convergent-divergent channel is studied numerically. The free stream is supersonic and parallel to the lower wall of channel. Solutions of the unsteady Reynolds-averaged Navier-Stokes equations are obtained with an open-source finite-volume solver SU2. The solutions demonstrate an expulsion/swallowing of the shock waves with variation of the free-stream Mach number M_∞. Flow topology in the channel and in front of its entrance is discussed. The hysteresis of shock wave positions with variation of M_∞ is determined.**

***Index Terms*—supersonic intake, shock waves, instability, hysteresis**

I. Introduction

Transonic airflow in bent channels is of practical interest in view of its application to the design of advanced aircraft intakes. A conventional intake consists of a convergent part, which lies upstream of the throat section, and a divergent part downstream of the throat. In the design regime of operation, there is a train of oblique shocks in the convergent part of the intake, where the flow is supersonic, and a terminal shock immediately downstream of the throat [1]. For low contraction inlets, this regime can be started by increasing the free-stream Mach number M_∞ up to a value that exceeds a Kantrowitz limit M_{start} [2]. After that, if M_∞ turns to decrease, then the terminal shock moves upstream and, at some value $M_{unstart} < M_{start}$, it is abruptly expelled from the intake. In the band $M_{unstart} < M_\infty < M_{start}$ there is a flow hysteresis, whose existence was explained in classical works on the basis of quasi-one-dimensional equations governing mass flow rate and stagnation temperature across the shock [3], [4].

The existence of a hysteresis must be taken into account in supersonic and hypersonic vehicles design, as different flow fields in the same flight conditions may essentially influence the fuel combustion and aerodynamic performance of the flying vehicle. In the last decade, the intake start/unstart was studied numerically and experimentally in a number of papers. For a Busemann supersonic biplane, numerical simulations showed that the width M_{start} — $M_{unstart}$ of the hysteresis band is 0.54 [5], [6]. Experimental studies of 3D biplane models [7] demonstrated that the biplane starts at lower Mach numbers than those predicted by 2D computations.

Li *et al.* [8] tested various flow characteristics in the intake starting process by using a high speed Schlieren system. Contraction ratio limits for the self-start were obtained, and the leading edge bluntness was shown to play an important role in the process.

Bravo-Mosquera *et al.* [9] performed analytical and numerical studies of a supersonic intake efficiency in on-design and off-design conditions. Meanwhile, the authors did not pay proper attention to the hysteresis phenomenon.

The nature of flow hysteresis in bent channels/intakes was discussed in [10] and [11], where the hysteresis was associated with an unstable interaction of shock waves with the region of abrupt acceleration over the convex wall of channel.

In the present paper we use SU2 solver for the study of the 2D turbulent flow hysteresis in bent channels with supersonic conditions at both the entrance and exit. The obtained results are compared to ones calculated using ANSYS CFX commercial solver.

II. Formulation of the problem

The lower wall of the channels under consideration is a convex corner given by the expressions as follows:

$$\begin{array}{ll} y(x) = 0 & \text{at} \quad 0 \le x \le 1.3, \\ y(x) = -(x-1.3)\tan 16^\circ & \text{at} \quad 1.3 < x \le 1.5, \end{array} \tag{1}$$

where (x, y) are dimensional Cartesian coordinates in meters. The profile of the upper wall/cowl of channel 1 is a rectangle of thickness 0.006, whose inner side is given by the formula

$$y(x) = 1 - (x-0.4)\tan 7^\circ \quad \text{at} \quad 0.4 \le x \le 2, \tag{2}$$

see Fig. 1. The inlet boundary of the computational domain is set at $x = 0$, $0 < y < 5$. The upper boundary is a horizontal segment $y = 5$, $0 \le x \le 2$ placed at a height of 5 in order to eliminates its influence on the flow field between the cowl and lower wall.

The outlet boundary is constituted by the exit of channel and a segment connecting the right upper corner $x = 2$, $y = 5$ of the computational domain and a point located on the upper surface of the cowl at $x = 0.8$. The lower wall of channel 2 is again determined by (1). Meanwhile the profile of cowl is a triangle, not rectangle, with the inner side (2); therefore, the cowl leading edge is sharp. The free stream is uniform and parallel to the x-axis so that the x- and y-components of

978-1-6654-1291-9/20/$31.00 ©2020 IEEE
DOI 10.1109/ISPRAS51486.2020.00034

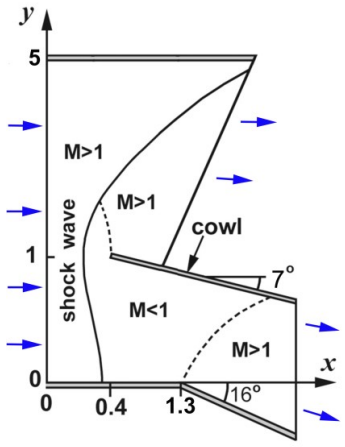

Fig. 1. Schematic of the computational domain.

the flow velocity on the left boundary of the computational domain are:

$$U_\infty = M_\infty a_\infty, \quad V_\infty = 0 \quad \text{at} \quad x = 0, \quad 0 \le y \le 5, \qquad (3)$$

where $M_\infty > 1$. Also we prescribe on the left boundary the static pressure $p_\infty = 5 \times 10^4$ Pa or $p_\infty = 2.5 \times 10^4$ Pa, a turbulence level of 1%, and static temperature $T_\infty = 250$ K which determines the sound speed $a_\infty = 317.02$ m/s. The outlet is endowed with a condition of the supersonic flow regime. The no-slip condition and vanishing heat flux are imposed on the walls. Initial data are either parameters of the free stream or a flow field calculated for a different free-stream Mach number. The air is treated as a perfect gas whose specific heat at constant pressure is 1004.4 J/(kg K) and the ratio of specific heats is 1.4. We adopt the value of 28.96 kg/kmol for the molar mass, and use the Sutherland formula for the molecular dynamic viscosity. Free-stream Mach numbers under consideration lie in the range $1.5 \le M_\infty \le 1.7$; therefore, the Reynolds number based on the middle of this range and length of 1 m is 2.2×10^7 and 1.1×10^7 for two above mentioned values of p_∞, respectively.

III. Numerical methods

Solutions of the unsteady Reynolds-averaged Navier-Stokes equations (URANS) were obtained with a SU2 open-source finite-volume solver developed by Prof. Alonso's and Dr. Palacios' groups at Stanford University along with a few other groups over the world (https://su2code.github.io) [12]. The solver is based on a method of lines, in which the governing equations are discretized in space and time separately. This decoupling of space and time allows for the selection of different types of schemes for the spatial and temporal integration. Spatial integration is performed using the finite volume method, while integration in time is achieved through several available explicit and implicit methods. For time-accurate calculations, we used a dual time-stepping approach. The global time steps of 2×10^5 s ensured the root-mean-square CFL number (over mesh cells) smaller than 3. To close the system of URANS equations, we used a Spalart-Allmaras turbulence model, which is known to reasonably predict aerodynamic flows with boundary layer separations [13]. The meshes were generated with package Gmsh [14]. Computational meshes were constituted by quadrangles in 35 layers on the walls and by triangles in the remaining region. The non-dimensional thickness y^+ of the first mesh layer was less than 4. The total number of mesh cells was about 2×10^5. Some test calculations were performed with the doubled number of mesh elements. We also varied the thickness of the lower layer of the mesh. These changes of the mesh actually did not influence the numerical solutions.

We used SU2 release 7.0.0 "Blackbird". The Courant-Friedricks-Levy (CFL) number of finest grid was less than 100. The FGMRES algorithm proposed by Saad [15] was chosen for the linear solver for implicit formulation. Minimum error of the linear solver for the implicit formulation was equal to 10^{-10}. Jameson-Schmidt-Turkel (JST) scheme [16] was used for convective terms. We employed the slope limiter proposed by Venkatakrishnan [17].

For a comparison, we calculated solutions of the problem using the commercial ANSYS-15 CFX finite-volume solver of second-order accuracy in space and time. The solver is based on a high-resolution discretization scheme by Barth and Jespersen [18] for convective terms. An implicit backward Euler scheme was employed for the accurate time-stepping. The SU2 2D mesh was transformed into a 3D mesh, whose lateral size was equal to one element. The transformed mesh is in the TGrid / Fluent format [19], which is suitable for the calculation in the package Ansys CFX.

IV. Results and discussion

First, the problem was solved at $M_\infty = 1.6$ using the uniform free stream (3) for initialization of the solution. Computations showed a convergence of the mean parameters of turbulent flow to a steady state in less than 0.2 s. The obtained flow field exhibits an oblique shock SW which propagates from the cowl downstream and downward, see Fig. 2a.

The shock is reflected from the lower wall ahead of the corner. Such a flow pattern, in which a shock system reaches the throat of channel, is called hereafter the flow regime with swallowed shocks. In order to trace streamwise positions of SW, we will plot the coordinates x_s of its intersection with the horizontal line $y = 0.25$, which is located above the boundary layer.

Using the solution obtained at $M_\infty = 1.6$, we solved the problem for smaller M_∞ step-by-step, as indicated on curve 1 in Fig. 3. At each step, initial conditions were parameters of the flow field obtained for the previous value of M_∞. As seen, the coordinate x_s of SW gradually decreases when M_∞ decreases from 1.60 to 1.528, and the flow regime with swallowed shocks persists.

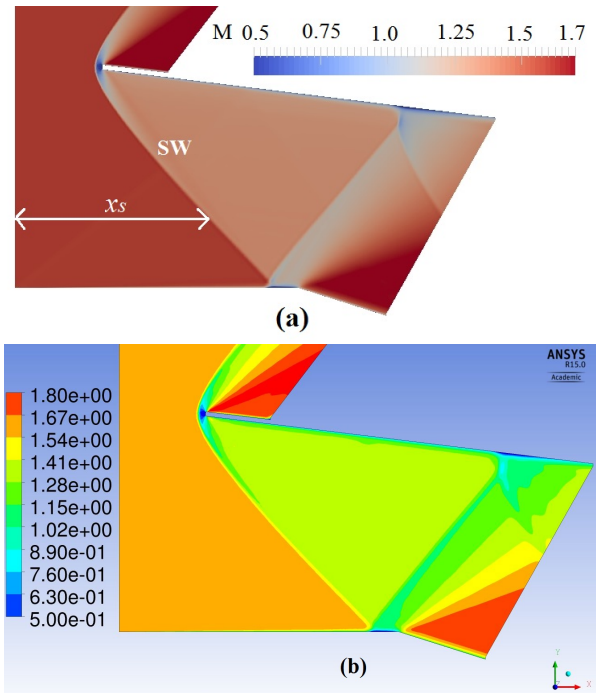

Fig. 2. Mach number contours in channel 1 at M$\infty = 1.6$, the flow regime with swallowed shocks: (a) Computations with SU2, (b) computations with ANSYS CFX-15 .

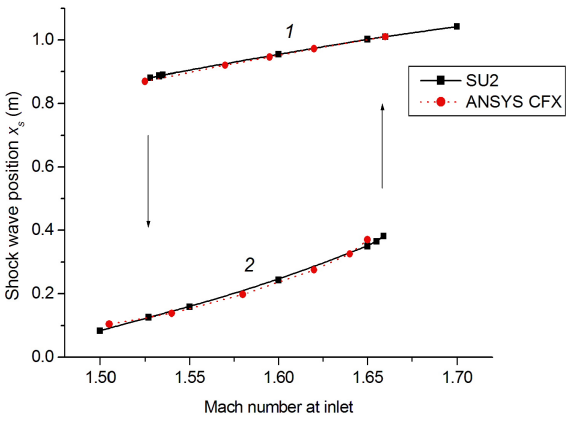

Fig. 3. Coordinate $x_s$of the shock wave SW versus the free-stream Mach number for channel 1. Solid curves: computations with SU2; dashed curves: computations with ANSYS CFX. Spalart-Allmaras turbulence model.

If M$_\infty$ is further decreased to 1.527, then computations show an abrupt expulsion of SW from the channel, accompanied by a jump of x_s to lower values and a transition from curve *1* to curve *2* in Fig. 3. After that if M$_\infty$ turns to increase from 1.5 to 1.60, then SW shifts downstream, and x_s gradually increases from 0.084 to 0.243; the obtained flow field is shown in Fig. 4. Further increase of M$_\infty$ to 1.659 is accompanied by a gradual increase in x_s, see curve *2* in Fig. 3. Meanwhile an increase of M$_\infty$ to 1.66 triggers a jump of SW to the position $x_s = 1.02$ and transition to the regime with swallowed shocks.

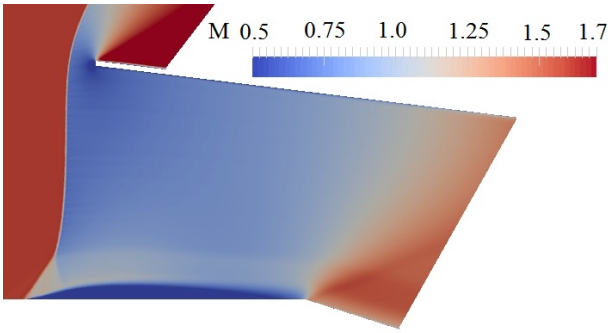

Fig. 4. Mach number contours in channel 1 at M$_\infty = 1.6$, the flow regime with the expelled shock SW. Computations with SU2.

A comparison of the solid and dashed curves displayed in Fig. 3 shows good agreement of the results obtained using SU2 and ANSYS CFX solvers.

Computations of the problem at the halved pressure p_∞ given at the inlet boundary and, consequently, halved Re, revealed only insignificant distinctions of the solutions from those demonstrated above. The employment of a $k-\omega$ Shear Stress Transport turbulence model also showed minor distinctions from the results discussed above, see Fig. 5.

Fig. 6 shows the coordinate x_s of SW as a function of M$_\infty$ calculated for channel 2 using the Spalart-Allmaras turbulence model.

Due to the sharpness of the edge of cowl, the shock SW is attached to the edge. That is why SW is shifted downstream to the exit as compared to SW in channel 1 at the same M$_\infty$. As a consequence, the hysteresis created by curves *2* and *3* in Fig. 6 resides at smaller values of M$_\infty$ than that detetmined by curve *1*.

V. Conclusion

Calculations of the transonic flow in a bent channel using a freely distributed SU2 package revealed the existence of a hysteresis in a certain range of Mach numbers given at the inlet of the channel. The boundaries of the hysteresis range are weakly dependent on the Reynolds number in the range from 1.1×10^7 to 2.2×10^7. A comparison of the solutions obtained using SU2 and Ansys CFX with Spalart-Allmaras and $k-\omega$ SST turbulences models showed that the solutions are close to each other. The boundaries of the hysteresis range for channel with sharp edge of the cowl are shifted to the smaller

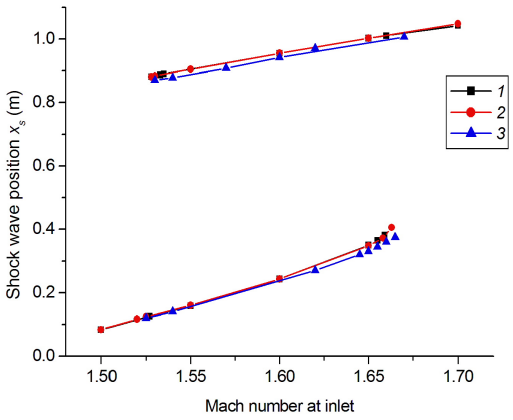

Fig. 5. Coordinate $x_s$of the shock wave SW versus the free-stream Mach number for channel 1. *1* — SU2, $p_\infty = 50000$ Pa, Spalart-Allmaras turbulence model; *2* — SU2, $p_\infty = 25000$ Pa, Spalart-Allmaras turbulence model; *3* — Ansys CFX, $p_\infty = 50000$ Pa, $k-\omega$ SST turbulence model.

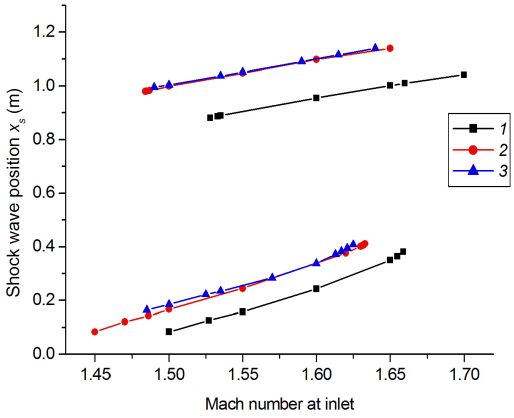

Fig. 6. Coordinate x_s of the shock wave SW versus the free-stream Mach number for channels 1 and 2. *1* — SU2, channel 1; *2* — SU2, channel 2; *3* — Ansys CFX, channel 2, $p_\infty = 50000$ Pa.

inflow Mach number in comparison to the channel with blunt edge of the cowl.

Acknowledgments

This research was performed using computational resources provided by the Computational Center of St. Petersburg State University: http://www.cc.spbu.ru/en

References

[1] P. M. Sforza, Theory of Aerospace Propulsion. Waltham: Academic Press, 2012.

[2] A. Kantrowitz and C. Donaldson, “Preliminary Investigation of Supersonic Diffusers”, National Advisory Committee for Aeronautics, Advanced Confidential Report L5D20, Langley Memorial Aeronautical Laboratory, 19 Langley Field, VA, 125, U.S.A. 1945. https://archive.org/details/preliminaryinves00lang. Accessed 20 Sep 2020.

[3] H. Daneshyar, One-dimensional Compressible Flow: Thermodynamics and Fluid Mechanics Series, Pergamon, Oxford, 1976.

[4] P. Hill and C. Peterson, Mechanics and Thermodynamics of Propulsion Systems (2nd Ed.), Addison-Wesley Pub. Ltd. 1992.

[5] K. Kusunose, K. Matsushima and D. Maruyama, “Supersonic biplane A review,” Progress in Aerospace Sciences, 47, pp. 53-87, 2011

[6] R. Hu, A. Jameson and Q. Wang, “Adjoint based aerodynamic optimization of supersonic biplane airfoils”, AIAA paper 2011-1248, 2011.

[7] H. Yamashita, N. Kuratani, M. Yonezawa, T. Ogawa, H. Nagai, K. Asai and S. Obayashi, “Wind tunnel testing on start/unstart characteristics of finite supersonic biplane wing,” Int. J. Aerosp. Eng, Article ID 231434, 2013.

[8] Z. Li, B. Huang and J. Yang, “A novel test of starting characteristics of hypersonic inlets in shock tunnel,” AIAA paper 2011-2308, 2011.

[9] P. D. Bravo-Mosquera, H. Muñoz, C. Darío. and F. M. Catalano, “Analytical and numerical design of a mixed-compression air intake for a supersonic fighter aircraft.” 1o SiPGEM 1o Simpòsio do Programa de Pós-Graduação em Engenharia Mecânica, Escola de Engenharia de São Carlos Universidade de São Paulo, 12 e 13 de setembro de 2016, São Carlos - SP, 2016

[10] A. Kuzmin, “Transonic flow instability in the entrance region of a channel with breaks of walls,” Arch. Appl. Mech. Vol. 87, pp. 1269–1279, 2017. DOI 10.1007/s00419-017-1248-7

[11] K. V. Babarykin, A. G. Kuzmin, A. N. Ryabinin, “Transonic flow bifurcanion in a channel with a break wall,” Vestnik SPbSU. Mathematics. Mechanics. Astronomy. Vol. 4 (62), issue 1, pp. 104-112, 2017. DOI: 10.21638/11701/spbu01.2017.112

[12] T. D. Economon, F. Palacios, S. R. Copeland, T. W. Lukaczyk and J. J. Alonso, “SU2: An Open-Source Suite for Multiphysics Simulation and Design,” AIAA J., Vol. 54, No. 3, pp. 828-846, 2016.

[13] P. R. Spalart and S. R. Allmaras, “A One-Equation Turbulence Model for Aerodynamic Flows,” AIAA Paper 92-0439, 1992.

[14] Ch. Geuzaine, J.-F. Remacle, Gmsh Reference Manual, 278 p., 2014. URL: http://geuz.org/gmsh/doc/texinfo/gmsh.pdf. Accessed 20 Sep 2020.

[15] Y. Saad, “A flexible innerouter preconditioned GMRES algorithm,” SIAM J. Sci. Comput. Vol. 14, pp. 461-469, 1993.

[16] A. Jameson, W. Schmidt and E. Turkel, “Numerical Solutions of the Euler Equations by Finite Volume MethodsUsing RungeKutta Time-Stepping Schemes,” AIAA paper 81-1259, 1981.

[17] V. Venkatakrishnan, “On the accuracy of limiters and convergence to steady state solutions,” AIAA paper 93-06680. 1993.

[18] T. J. Barth and D. C. Jespersen, “The design and application of upwind schemes on unstructured meshes,” AIAA paper 89-0366, 1989.

[19] TGrid 5.0 Users Guide. Lebanon: ANSYS, Inc., 281 p. 2008.